Environ. Sci. Technol. **2010,** *44,* 1116–1122

Oxidative Decolorization of Acid Azo Dyes by a Mn Oxide Containing Waste

CATHERINE E. CLARKE,*,† FILIP KIELAR,‡ HELEN M. TALBOT,§ AND KAREN. L. JOHNSON||

Department of Earth Sciences, Stellenbosch University, South Africa, School of Engineering, Durham University, South Road, Durham, DH1 3LE, United Kingdom, Civil Engineering and Geosciences, Newcastle University, United Kingdom, Universita degli Studi del Piemonte Orientale Amedeo Avogadro, Dipartimento di Scienze dell'Ambiente e della Vita, Alessandria

Received May 25, 2009. Revised manuscript received November 16, 2009. Accepted November 30, 2009.

A Mn oxide containing mine tailings, generated in the Kalahari Mn fields, has been shown to oxidatively breakdown acid azo dyes acid orange (AO) 7, acid red 88, acid red 151 and acid yellow 36 but not acid yellow 9. The total reducible Mn content of the tailings is 33%, of which 3% is hydroquinone extractable and thus easily reducible. The net oxidation state of the Mn within the tailings is 3+. Decolorization of AO 7 by the Mn tailings increases with decreasing pH. The decolorization mechanism is initiated on the hydroxyl group of AO 7 and proceeds via successive electron transfers from the dye molecule to the oxide surface resulting in the asymmetric cleavage of the azo bond. The reaction products have been identified as 1,2-naphthoquinone, 4-hydroxybenzenesulfonate, and coupling products involving 1,2-naphthoquinone and benzenesulfonate radicals. The AO 7: Mn(III) reaction stoichiometry has been tentatively calculated to be 1:3. The reaction shows longevity with 95% decolorization still observed after 60 days of dye replenishment. Further breakdown of 1,2-naphthoquinone and 4-hydroxybenzenesulfonate was not observed, thus these compounds are considered to be the terminal reaction products of the AO 7- Mn tailings reaction.

Introduction

Textile industries produce large volumes of wastewater polluted with dyes. It is estimated that between 10 and 15% of manufactured dyes are lost in wastewater streams (*1*). Within the compounds manufactured as dyestuffs, azo dyes represent the largest class of dyes (*2*). The release of azo dyes into the environment is undesirable not only for obvious aesthetic reasons, but also because of the toxic and mutagenic properties of many dyes (*3*). The removal of azo compounds from textile waste streams is a pertinent issue in water treatment and currently there is no single, economically attractive treatment that can effectively decolorize dyes (*4*). Anaerobic treatment causes rapid decolorization but generally generates breakdown products which are more carcinogenic than the parent molecules (*4*). Advanced oxidation processes such as ozonation (*5*), Fenton's reagents (*6*) and photocatalysis using UV radiation (*7*) have shown the capacity to oxidatively decolorize dye solutions. The major drawbacks of advanced oxidation processes are the high capital input requirements and running costs.

White rot fungi are able to oxidatively decolorize a number of acid azo dyes via peroxidase mediated reactions (*8–12*). The active oxidant in many peroxidase mediated reactions is complexed Mn(III) ions (*13*). The chelated Mn(III) acts as a diffusible low molecular weight oxidant capable of oxidizing alkyl, aromatic, and phenolic substrates (*14*).

Despite Mn playing a key role in certain peroxidase mediated dye oxidation, little is known of the decolorization capacity of Mn (III or IV) in its oxide form. Observations of dye decolorization by Mn oxides have been made (*15–18*), however, little is known about the reaction mechanisms involved and the breakdown products formed.

Although the oxidizing potential of Mn (III and IV) oxides is widely recognized the use of Mn oxides as an effluent treatment technique has gained little recognition. The authors have identified significant quantities of Mn oxide-containing mine waste in the form of mine tailings material. The fine (<2 mm) Mn tailings are generated in great volumes during the mining operations of the Kalahari manganese fields (KMF) situated in the Northern Cape Province of South Africa. The KMF represent the largest known Mn ore body in the world and contains up to 135 different minerals, 59 of which are Mn bearing (*19*).

The Mn tailings are generated during the ore extraction and crushing operations and have undergone no chemical processing thus the Mn oxides contained in the tailings are derived directly from the ore deposit. This study demonstrates the potential of the Mn tailings to oxidatively decolorize a number of acid azo dyes (Structures given in Figure S1 of the Supporting Information). The decolorization reaction for the model dye AO 7 is discussed in detail.

Materials and Methods

Manganese tailings material was collected by taking composite samples from the tailings dumps. The tailings were dry at the time of collection. Details of the Mn tailings' mineralogical, physical and chemical characterization are given in the Supporting Information.

Decolorization Reactions. In this work, the term decolorization is used to describe the loss of absorbance in the visible region (400−700 nm) of a UV−visible spectrum. Percentage decolorization is calculated using the following equation:

$$\%\ \text{decolorisation} = (1\text{-AA/AB})x100$$

Where AA is the absorbance after and AB is the absorbance before the reaction, measured at the λ_{max} of the dye in the visible region (*20*)

Five azo dyes (purchased from Sigma-Aldrich), acid yellow 9 (AY 9), acid red 88 (AR 88), acid red 151 (AR 151), acid yellow 36 (AY 36) and acid orange 7 (AO 7) were reacted with the Mn tailings in a pH 4 acetate buffer using a batch procedure. Dye stock solutions at a concentration of 0.14 mM were prepared in a 0.2 M, pH 4 acetate buffer. A 40 mL volume of stock solution was added to 2 g of tailings material, weighed out into 50 mL centrifuge tubes. These suspensions

* Corresponding author address: Department of Earth Sciences, Stellenbosch University, P/Bag X1, Matieland, 7602, South Africa; phone: (+27218083117); e-mail: cdowding@sun.ac.za.
† Department of Earth Sciences, Stellenbosch University.
‡ Universita degli Studi del Piemonte Orientale Amedeo Avogadro, Dipartimento di Scienze dell'Ambiente e della Vita.
§ Civil Engineering and Geosciences, Newcastle University.
|| School of Engineering, Durham University.

10.1021/es902305e

Published on Web 01/13/2010

were agitated on a reciprocal shaker set at 250 rpm. In all cases, controls and blanks were prepared by omitting the Mn tailings and the dye solution, respectively. At various time intervals, specified in the corresponding figures, samples were removed and centrifuged at 3000 rpm for 5 min. The supernatants were analyzed using UV−visible spectrometry (Varian Cary 50).

The effect of pH was established by reacting the tailings with AO 7 at pH 9; 7; 5; 4; and 3. Samples were prepared by weighing 2 g tailings material into 50 mL centrifuge tubes and adding 20 mL deionized (DI) water. The pH of this slurry was adjusted and held constant by addition of 0.1 M HCl using a Metrohm 785 titrino autotitrator. Once the desired pH was reached 2 mL of 1000 ppm dye stock solution (prepared in DI water) was added to the suspension. After reacting for 1 h, all sample volumes were adjusted to 40 mL using DI. Samples were shaken for 10 s, centrifuged and the supernatants filtered before analysis with UV−visible spectroscopy and High Performance Liquid Chromatography. Soluble Mn concentrations were measured in the decolorized dye solutions as well as in a series of pH adjusted blank solutions using atomic absorption spectroscopy (AAS) on a Varian SpectraAA 220FS spectrometer. Reaction rates were determined at pH 4 and 6 by reacting the tailings with acetate-buffered AO 7 dye solutions and blanks. Aliquots were extracted and filtered at increasing time intervals and the Mn concentration determined using AAS. The dye related Mn release ($[Mn]_{diss}$) was calculated by subtracting Mn release in the dye treatments from Mn release in the blanks.

Liquid Chromatography. High Performance Liquid Chromatography (HPLC) was conducted using a Perkin-Elmer Series 200 fitted with a Genesis, C-18 column (4.6 × 250 mm) containing 4 μm packed particles (Alltech, Deerfield, Germany). Acetonitrile and 0.03 M, pH 7.7 ammonium carbonate buffer were used as eluents. The pump program was set as follows: isocratic 20% acetonitrile: 80% buffer held for 2 min; grading to 100% acetonitrile over 10 min and held at 100% for 7 min. The chromatograms were recorded at 254 and 484 nm. The diode array detector allowed for concomitant recording of spectra from 200 to 600 nm. Dye concentrations were determined from peak area-concentration curves, plotted for a series of concentration standards (1.3×10^{-6} M to 1.1×10^{-4} M).

Liquid chromatography−mass spectroscopy (LC−MS) was conducted on two different systems depending on instrument availability. In the first system, separation was accomplished using a Surveyor HPLC system (ThermoFinnigan, Hemel Hempstead, UK) fitted with the same column described above. LC−MS^n was performed using a Finnigan LCQ ion trap mass spectrometer equipped with an electrospray ionization interface (ESI) source operated in positive or negative ion mode.

In the second system reversed-phase HPLC was accomplished using a Surveyor HPLC system (ThermoFinnigan, Hemel Hempstead, UK) fitted with a Phenomenex, C-18 column (2.00 mm × 150 mm) containing 3 μm packed particles. LC−MS was performed using a ThermoFinnigan LTQ ion trap mass spectrometer equipped with an ESI source operated in positive or negative ion mode. Details of the LC−MS settings for both systems are provided in the Supporting Information. The major difference between the two systems described above, is the first system allowed secondary fragmentation patterns to be obtained of the most intense ion detected in the initial scan, while in the second system only one scan of the intact parent ions was obtained.

Results and Discussion

Tailings Characterization. The mineralogy of the KMF has been well characterized (*19*), thus an extensive mineralogical study was not required. The clay phase of the tailings is likely to be the most reactive in geochemical reactions, thus a brief mineralogical survey was conducted of the clay fraction extracted from tailings. X-ray diffraction data along with other chemical and physical properties of the tailings is provided in Table S1 of Supporting Information. The major mineral phases identified include manganite, braunite, bixbyite, hausmannite, birnessite, todorokite, hematite, and calcite all of which have been identified within the KMF (*19*). Although Mn carbonate minerals were not identified in the clay extract, these minerals (e.g., kutnahorite and rhodochrosite) have been identified in the KMF by previous workers (*19*). The BET surface area analysis indicated a very low surface area ($2.4\ m^2 \cdot g^{-1}$), which relates to the coarse texture of the material (83.3% sand size fraction). Textural differences within the tailings are a result of mechanical crushing during ore excavation and milling processes. Major and selected trace element concentrations measured in an aqua regia extract are given in Table S2 (Supporting Information). The low trace element concentrations in the Mn tailings suggests that the material would be suitable for water treatment, as it will not release unacceptable levels of toxic metals into solution.

TABLE 1. Percentage Decolorization of 5 Acid Azo Dyes Reacted with the Mn Tailings for 2 and 24 h in a pH 4 Acetate Buffer

dye	% decolorization (2 h)	% decolorization (24 h)
acid orange 7	42	91
acid red 88	94	97
acid red 151	97	97
acid yellow 36	93	96
acid yellow 9	0	0

Despite the low surface area, the tailings show a high reactivity with an easily reducible (hydroquinone (HQ) extractable) phase of 3% (w/w). The total reducible (dithionite citrate (DC) extractable) phase is 33.3%. The high HQ and DC extractable contents of the tailings suggest that the material will have "quick" and "slow" release oxidizing capacity. The difference between the Mn concentration measured in the aqua regia extract (38%; Table S2) and that measured in the DC extract represents the Mn phase associated with carbonates and aqua regia soluble silicates. The O/Mn ratio is 1.5 indicating an average Mn oxidation state of 3+. The pH of the tailings is 8.8 and is likely to be buffered by the carbonate minerals in the material.

Attempts to determine the surface charge potentiometrically were unsuccessful on the whole tailings (<2 mm) due to the pronounced buffer capacity, which required large volumes of acid to adjust the pH below pH 4. Potentiometric titration of the clay phase was also unsuccessful and a discrete point of zero charge (PZC) could not be determined. Instead, a flocculation technique was employed and visual observation made to determine the pH at which the clay phase began to flocculate (Figure S2 of the Supporting Information).

Amphoteric oxides have been shown to aggregate near the pH of their PZC (*21*) where the electrostatic repulsion between the particles is negligible. This may be expected to be a discrete point for a single mineral phase, but for a mineral compilation like the Mn tailings flocculation might be expected to occur over a range of pH values. Clay particles of the Mn tailings aggregate below pH 4, therefore we assume that the PZC for the tailings is below pH 4. This seems reasonable based on the low PZC often reported for Mn oxides (*22*).

Decolorization Reactions. The percentage decolorization of the five azo dyes after reaction with the tailings for 2 and 24 h is presented in Table 1. The UV−Visible spectra are provided in Figure S3 (Supporting Information). Acid azo

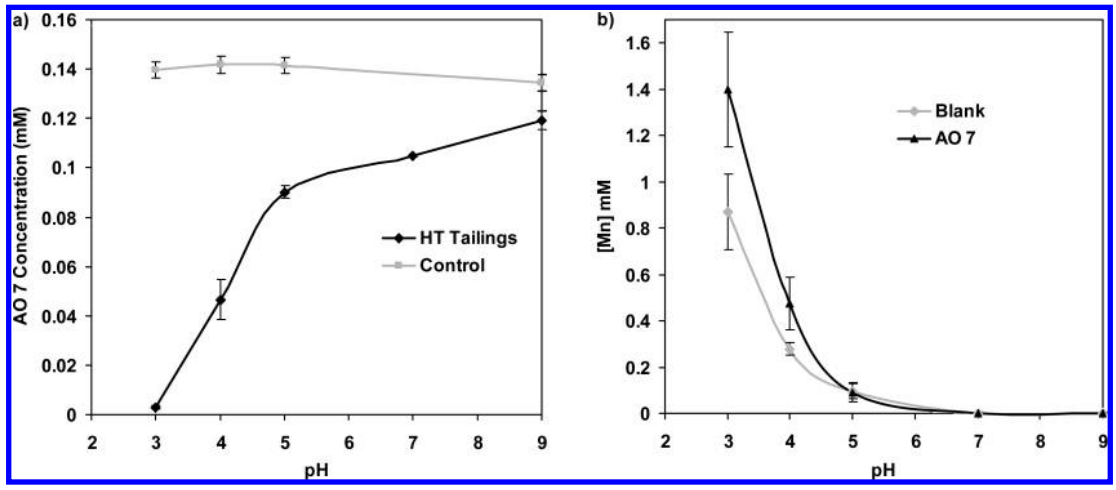

FIGURE 1. Concentration (mM) of (a) AO 7 and (b) soluble Mn after reacting the Mn tailings (HT tailings) for 1 h with 0.14 mM AO 7 at pH 3, 4, 5, 7, and 9 presented with Mn release from pH adjusted blank samples.

dyes AR 88, AR 151, AY 36, and AO 7 all show near complete (>90%) decolorization after reaction with the Mn tailings for 24 h (Table 1). There is no color removal of AY 9 (Table 1). Acid yellow 9 is one of the most recalcitrant of the azo dyes due to the arrangement of electron withdrawing substituents (*23*). The UV−Visible spectra of the decolorized supernatants from AR 88, AR 151, AY 36, and AO 7 show new peaks in the UV region which persist after 28 days of reaction (Figure S3 of the Supporting Information), suggesting that alteration of the dye molecules had taken place rather that color removal via sorption of the dyes to the tailings surface. The structures of AR 151, AR 88, and AO 7 all contain an OH functional group on the aromatic ring (Figure S1 of the Supporting Information), whereas AY 36 contains a phenylamine group. Thus, it is likely that any transformations of AY 36 will follow a chemical pathway different to that of the other dyes as will be shown in a future communication.

Oxidative Breakdown of Acid Dye AO 7. Removal of color from a dye solution can either be as a result of sorption reactions or transformation of the parent molecule to colorless breakdown products. The aim of this section was to establish the processes involved in color removal of AO 7 by the Mn tailings. Acid orange 7 was chosen as a model dye as it displays the "core-structure" of a number of commercial dyes and thus has similar physiochemical properties of the more complex dye compounds (*24*).

pH Treatments. The pH range investigated spanned from pH 3 to 9. This pH range was chosen because the pH of the tailings is close to 9 and acid dyes are applied in organic acid buffers thus textile effluents are often acidic. A set of controls (pH adjusted AO 7 solutions) were assessed by UV−Visible spectroscopy to establish any pH-related color changes or flocculation of the original dye over this pH range. No pH-dependent wavelength shifts or concentration differences were observed in the UV−Visible spectra of the controls.

A plot of AO 7 concentration for samples reacted with the Mn tailings for 1 h at pH 3, 4, 5, 7, and 9 is given in Figure 1a. The concentration of AO 7 in solution decreases as a function of pH when reacted with the Mn tailings. Dye removal is most pronounced below pH 5, and increases linearly as pH decreases with 95% color removal achieved at pH 3. Figure 1b shows the Mn concentration measured in the decolorized dye and blank solutions. In both the blank and treatment solutions, soluble Mn concentrations were below detection limit above pH 7, but at lower pH soluble Mn increases exponentially. This pH-dependent Mn release from the blank samples is expected and can originate through a number of factors including, dissolution of Mn carbonate minerals, reductive dissolution of Mn oxides as the redox potential of the oxides increases and/or release of Mn(II) ions housed in the Mn oxide mineral lattice via proton promoted dissolution (*25*). There is large variation in the Mn release both in the blank and the dye treatment below pH 4 and at pH 3 the difference between the Mn release in the blank and dye treatment just fails a significance test at a 5% confidence interval ($P = 0.059$). The reason for this large variation most likely stems from the heterogeneous nature of the tailings and it was noted that different acid volumes and reaction times were needed to obtain the starting pH conditions in repeat experiments. The UV−Visible spectra measured at each pH are given in Figure S4 of the Supporting Information.

The pH 4 treatment was analyzed by HPLC to establish whether oxidative or sorption reactions were responsible for the progressive increase in decolorization in increasingly acidic solutions. The chromatogram is shown in Figure 2. The peak at 13.8 min was identified in both the blank (DI water) and the treated sample as a plastisizer and the small peak at 9.7 min was present in the dye control thus these peaks will be ignored in the subsequent discussion.

Five compounds were observed following chromatographic separation of the pH 4 treatment. The peak at 10.2 min represents that of the parent compound, while the remaining four peaks represent breakdown products.

Previously 1,2-naphthoquinone (NQ), 4-hydroxybezenesulfonate (4HBS), and benzenesulfonate (BS) have been identified as breakdown products in the oxidation of AO 7 by the enzyme laccase (*11, 20*). The UV spectra and retention times of the NQ and 4HBS standards compare well with the 8.9 and 3.3 min peaks, respectively (Figure S5 of the Supporting Information), suggesting that theses compounds are breakdown products of AO 7 oxidation by the Mn tailings. The BS standard, although having a comparable retention time did not have a UV spectrum fitting that of the 2.3 min peak (Figure S5 of the Supporting Information) and thus its formation as a product cannot be confirmed by HPLC analysis. The small peak at 5.2 min was observed in the NQ standard and is assigned to quinone-hydroquinone equilibrium (*11*).The peak at 3.7 min gives a UV spectrum with a broad absorption band, this was assigned to one of the coupling products between 1,2-naphthoquinone and benzenesulfonate radicals discussed below.

To establish the effect of pH on reaction rate the tailings were reacted with AO 7 at pH 6 and 4 and $[Mn]_{diss}$ measured over time (Figure S6 of the Supporting Information). Manganese release is commonly used for kinetic determinations due to the difficulty of obtaining reductant sorption data (*26*). Initial release rates of 3×10^{-6} M·min^{-1} and 4×10^{-8} M·min^{-1} were measured for the pH 4 and pH 6 treatments, respectively. This demonstrates that reaction kinetics will

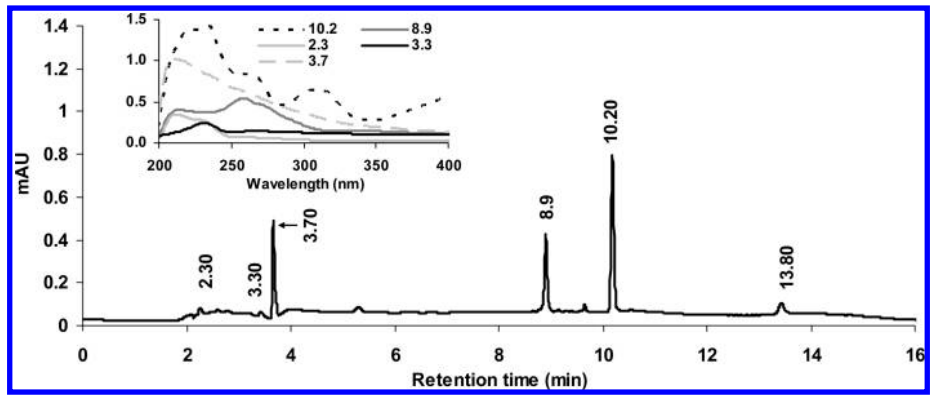

FIGURE 2. Chromatogram of the AO 7 solution after reaction with the tailings at pH 4 for 1 h. UV−Visible spectra corresponding to peaks at the various retention times shown in the inset.

TABLE 2. Mass Spectra Data of AO 7 and Degradation Products

compound no.	retention time[a] (min)	mode	MS *m/z* (% relative intensity)	MS^2 (% relative intensity)
I		ES−	173 (100); 198 (80); 196 (70); 137 (36)	NA
II	3.73	ES−	313 (100); 314 (22); 315 (10); 329 (5)	285 (100); 249 (17); 257 (5); 233 (7)
III	3.94	ES−	329 (100); 173 (90); 411 (40); 287 (34);	301 (100); 285 (52); 302 (30); 273 (7)
IV[b]		ES+	159 (100); 191 (45); 181 (31)	NA
V	7.65	ES−	327 (100); 500 (10); 329 (5)	171 (100); 247 (12); 156 (10)

[a] Excessive crusting on the ion transfer tube prevented the use of ammonium carbonate buffer in the LC−MS systems therefore retention times for HPLC and LC−MS data differ. [b] Compounds I (rt: 3.9 min) and IV (rt: 5.7 min) were identified using the second LC−MS system described in the methods section, thus retention times have not been included in the table.

contribute to the observed decolorization efficiency at low pH. Other factors influencing the reaction rate such as tailings surface area and dye concentration will be dealt with in a future paper.

From the above data, it is clear that the dye is reacting with the Mn oxides within the tailings to produce breakdown products and the reaction is enhanced as the pH is lowered. The influence of pH in the reaction between organic molecules and Mn oxides has been well established, with a decrease in pH facilitating oxidation of various organic compounds (*27–29*). These workers have attributed the increased oxidation of organic compounds by Mn oxides at lower pH to: (i) the decrease of the negative charge on the Mn oxide surface; (ii) positive charging of the organic molecule resulting in electrostatic attraction to the oxide surface; (iii) the increased redox potential of the MnO_2/Mn^{2+} couple; and (iv) enhanced removal of Mn^{2+} from the oxide surface, exposing new reactive sites. It is likely one or more of these pH-dependent influences are playing a role in the reaction between AO 7 and the Mn tailings. As discussed above, the Mn tailings have a PZC below 4. The pK_{a1} of AO 7 is 1, which corresponds to the protonation of the sulfonate group (*30*), therefore in the pH range of this study (3 to 9) the molecule will be negatively charged. This implies that any electrostatic attraction between the dye and the Mn oxide surface will be dependent on charge generation on the oxide surface. Sorption of AO 7 on other oxides (Ti, Fe, and Al oxides) has been shown to commence once the pH is lowered sufficiently to generate $M-OH_2^+$ groups on the oxide surface and increases linearly below the PZC of the oxide (*30*). Similar increases in sorption and thus oxidation are likely to occur with positive charge generation on mineral phases within the tailings.

Reaction and Polymerization Products Determined by LC−MS. The mass spectral data for AO 7 and its breakdown products is summarized in Table 2. Compound (V), measured in negative ion mode, represents the parent dye molecule (*m/z*: 327). The fragmentation pattern of the parent dye molecule is in good agreement with the fragmentation observed by Lopez et al. (*11*) for AO 7.

Four AO 7 degradation products were identified using LC−MS analysis. In addition to 4HBS and NQ (compounds I and IV, respectively) observed in the HPLC investigation, two additional products (compounds II and III) were identified. Compound II has been interpreted as being the coupling product of BS and NQ. Similarly, compound III has been identified as the polymerization product of the intermediate oxidation species and NQ. The presence of a NQ group in compounds II and III is supported by a loss of CO [M-28] from the major ions. Comparable polymerization products have been identified during enzymatic oxidation of AO 7 (*31*).

The proposed reaction mechanism for AO 7 oxidation by the Mn tailings is given in Scheme 1. The mechanism is similar to that proposed for peroxidase degradation mechanisms (*8, 11, 20, 31*). Electron transfer from the phenolic group to the Mn oxide generates a phenoxy radical which undergoes resonance rearrangement and additional electron transfer to generate a carbocation on the C-1 carbon of the naphthol ring. Nucleophilic attack by water generates an unstable tetrahedral complex resulting in the cleavage of the C−N bond yielding 1,2-naphthoquinone (IV) and (4-sulfophenyl)diazene. Although the latter compound was not detected in the current study, possibly due to its instability in the oxidative environment, it has been identified by Lopez et al. (*11*). Unstable diazene derivatives readily oxidize in the presence of oxygen to generate unstable phenyldiazene radicals (*32*). These phenyldiazene radicals in turn lose the azo linkage to yield N_2 and a phenyl radical (*33*). The phenyl radical can abstract a hydrogen radical from its surroundings to generate a stable phenyl compound (*12*), take part in coupling reactions with other oxidation products (*31*), or undergo further oxidation followed by nucleophilic attack by water to generate 4-hydroxybenzenesulfonate. Benzenesulfonate was not detected in the LC-MS or HPLC study, however, 4-hydroxybenzenesulfonate (I) and coupling prod-

SCHEME 1. Proposed Mechanism for the Oxidation of AO 7 by the Mn Tailings

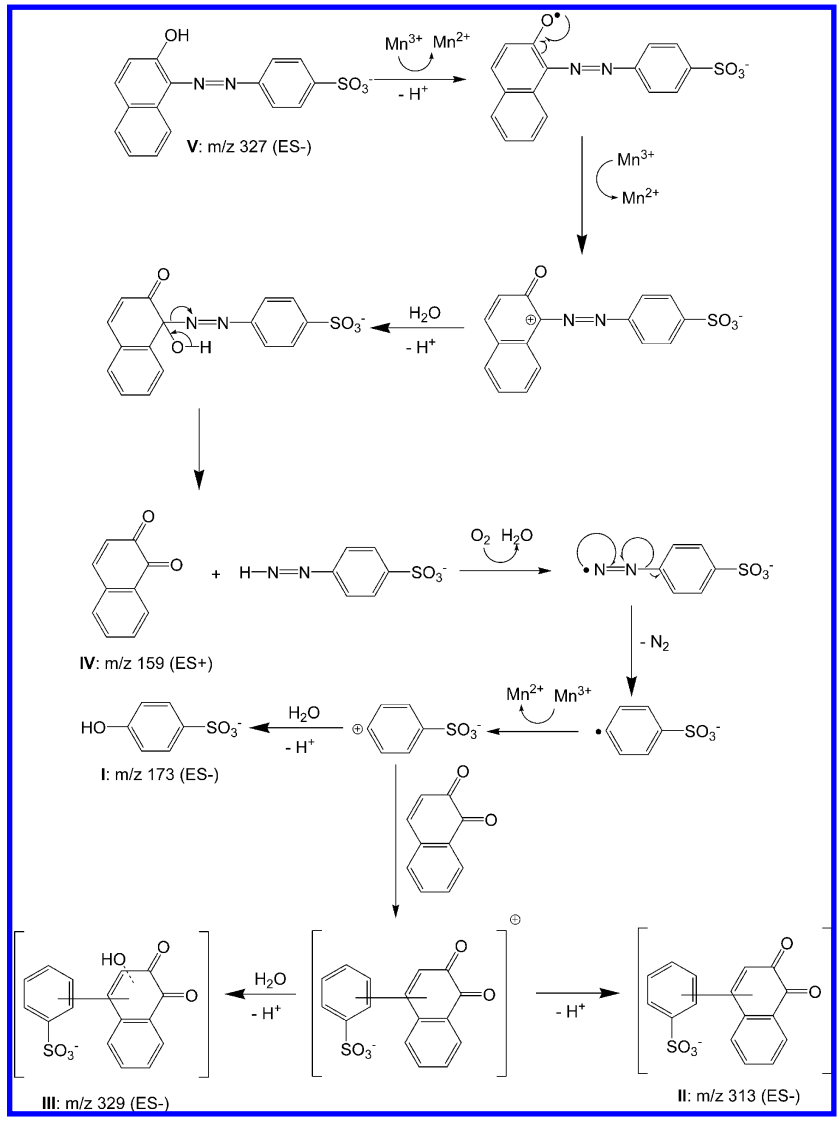

ucts (II and III) of benzenesulfonate and NQ were detected, suggesting that the latter two processes are occurring. This reaction mechanism suggests the asymmetric cleavage of the azo bond.

The mechanism presented in Scheme 1 involves three successive electron transfers. It has been established that the net oxidation state of the tailings is 3+, and the mineralogy shows a predominance of Mn(III) oxides. If this were the case, then the reaction would have a dye: Mn(III) reaction stoichiometry of 1:3 and 3 mols of Mn^{2+} would be expected to be generated from the breakdown of 1 mol of AO 7.

To assess the correlation between dye decolorization and Mn release, AO 7 was reacted with the tailings for 18 h in a pH 4 acetate buffer. Aliquots were collected periodically and analyzed for dye and Mn content. The relationship between percentage decolorization and $[Mn]_{diss}$ (Mn release additional to the blank), is given in Figure 3a. There is an initial increase in dye decolorization without concomitant Mn release, but after this, further decolorization is proportional to $[Mn]_{diss}$. The initial color decrease, without simultaneous Mn release suggests the dye is adsorbing to the tailings prior to the oxidation reaction. It is interesting to correlate the concentration of AO 7 as a function of $[Mn]_{diss}$ after the first sampling interval (i.e., not including the initial rapid dye removal) (Figure 3b). A linear correlation exists (R^2= 0.99) with a gradient of −0.32 giving an AO 7: Mn(III) reaction stoichiometry of 1:3 as suggested by the reaction mechanism above.

To establish whether 4HBS and NQ are the terminal products in the reaction, these 2 compounds were reacted with the tailings in a pH 4 buffer. No transformation of NQ or 4HBS was observed after 28 days reaction time, thus it is assumed that these two compounds and their coupling products are the final products of AO 7 oxidation and complete mineralization of the dye is not possible using the Mn tailings under the current experimental conditions. 1,2-Naphthoquinone is a colored product which explains why total color removal was never achieved.

Effluent treatment technologies are highly dependent on the longevity of the reactive surface. To establish if the Mn tailings can sustain the decolorization reaction over an extended period of time, a batch experiment was conducted in which the acetate buffered (pH 4) dye solutions were replenished daily and dye and Mn concentrations measured in the decolorized extracts. The decolorization and Mn release results are shown in Figure 4.

On days 1 and 2, the alkalinity of the tailings resulted in the pH drifting upward to 4.7 over the 24 h reaction period. Maximum decolorisation (95%) is reached on day 3 when the pH stabilized at 4. After 60 days of dye replenishment 95% decolorization was still being achieved illustrating the

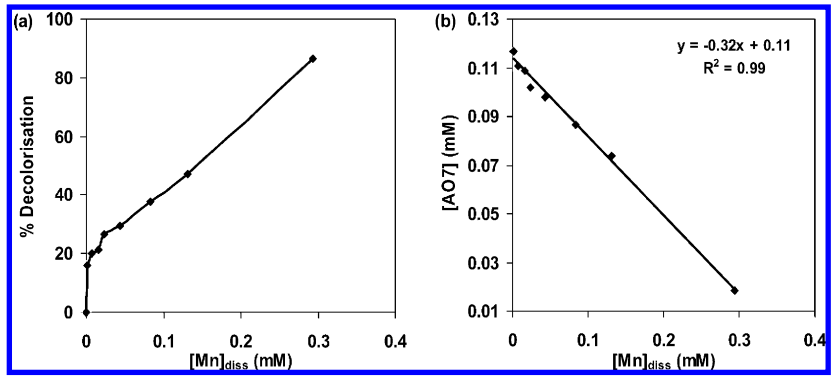

FIGURE 3. (a) Percentage decolorization of AO 7 plotted against $[Mn]_{diss}$ for a 0.14 mM AO 7 solution reacted with the Mn tailings (Solid:Liquid ratio 1:50) in a pH 4 acetate buffer over 18 h and (b) AO 7 concentration as a function of $[Mn]_{diss}$ excluding the first sampling interval (after 0.5 min).

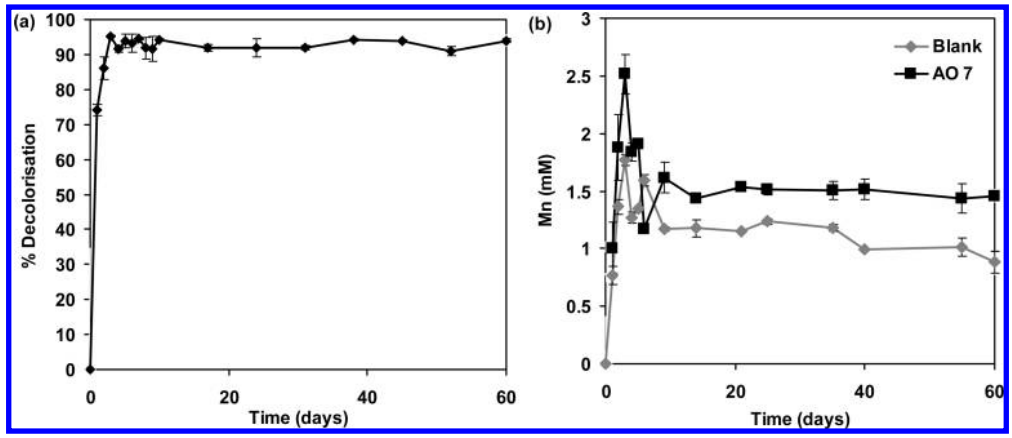

FIGURE 4. (a) Percentage decolorisation of AO 7 by a single measure of Mn tailings after daily replenishment of fresh dye stock solution (0.14 mM in pH 4 acetate buffer) and (b) Mn release measured in the blank and decolorized dye solution extracts from the tailings over this period.

longevity of the tailings oxidative capacity (Figure 4a). The initial spike observed in the Mn release of both the dye treatment and the blank (Figure 4b) is likley to result from dissolution of a carbonate or a highly labile Mn phase. After this initial spike, the Mn release stabilizes at 1.5 mM for the dye treatment and 1.1 mM in the blank.

Environmental Implications. The Mn tailings have shown the capacity to oxidatively decolorize acid azo dyes AO 7, AY 36, AR 88, and AR 151, but not the recalcitrant dye AY 9. The Mn oxide component of the tailings provides the oxidative potential for the reaction. The proposed mechanism for the decolorization of the dyes involves cleavage of the azo bond. As observed with many white rot fungi mediated dye decolorization reactions (*8, 10–12*), complete mineralization of the dyes was not achieved after reaction with the tailings. The reaction mechanism and terminal reaction products of Mn oxide-mediated dye decolorization are essentially the same as that proposed for enzymatic reactions. Unwanted coupling products were identified in this study and in enzyme mediated oxidations (*31*). By controlling the contact time between the oxidant and the dye, it may be possible to limit the coexistence of the different radical species thereby hindering the formation of some of the coupling products. The longevity of the decolorization reaction was demonstrated, which is essential for a viable treatment technology. A distinct disadvantage of using Mn oxides, to treat acid azo dyes lies in the release of soluble Mn, especially in acidic media. This released Mn would need to be recovered if this technology were to be useable. The reaction rate is dependent on pH and even at pH 4 dye removal rates of 3.9 $mg \cdot hr \cdot g^{-1}_{tailings}$ (based on a Mn:AO 7 reaction stoichiometry of 1:3) were calculated suggesting that dye removal may be too slow for a wastewater treatment technology. More information on reaction rates and impacts of auxiliary compounds, such as salts and organic acids, is needed before the viability of using the Mn oxide containing waste can be determined. These issues will be dealt with in a future communication.

Acknowledgments

This work was funded by the Engineering and Physical Science Research Council of the United Kingdom.

Supporting Information Available

Additional details of experimental methods and instrument setup, data pertaining to the Mn tailings and UV−visible spectral analysis of AY 9, AY36, AR 88, and AR 151 decolorization. This information is available free of charge via the Internet at http://pubs.acs.org/.

Literature Cited

(1) Zhao, X.; Lu, Y.; Hardin, I. Determination of biodegradation products from sulfonated dyes by Pleurotus ostreatususing capillary electrophoresis coupled with mass spectrometry. *Biotechnol. Lett.* **2005**, *27* (1), 69–72.

(2) Zollinger, H., *Color Chemistry - Syntheses, Properties and Applications of Organic Dyes and Pigments*; VCH Publishers: New York, 1987.

(3) Chung, K.-T.; Stevens, S. E.; Cerniglia, C. E. The Reduction of Azo Dyes by the Intestinal Microflora. *Crit. Rev. Microbiol.* **1992**, *18* (3), 175–190.

(4) dos Santos, A. B.; Cervantes, F. J.; van Lier, J. B. Review paper on current technologies for decolourisation of textile wastewaters: Perspectives for anaerobic biotechnology. *Bioresour. Technol.* **2007**, *98* (12), 2369–2385.

(5) Muthukumar, M.; Selvakumar, N. Studies on the effect of inorganic salts on decolouration of acid dye effluents by ozonation. *Dyes Pigments* **2004**, *62* (3), 221–228.

(6) Gutowska, A.; Kaluzna-Czaplinska, J.; Jozwiak, W. K. Degradation mechanism of Reactive Orange 113 dye by H_2O_2/Fe^{2+} and ozone in aqueous solution. *Dyes Pigments* **2007**, *74* (1), 41–46.
(7) Bandara, J.; Mielczarski, J. A.; Kiwi, J. 2. Photosensitized degradation of azo dyes on Fe, Ti, and Al oxides. Mechanism of charge transfer during the degradation. *Langmuir* **1999**, *15* (22), 7680–7687.
(8) Chivukula, M.; Spadaro, J. T.; Renganathan, V. Lignin Peroxidase-Catalyzed Oxidation of Sulfonated Azo Dyes Generates Novel Sulfophenyl Hydroperoxides. *Biochemistry* **1995**, *34* (23), 7765–7772.
(9) Cremonesi, P.; Cavalieri, E.; Rogan, E. One-Electron Oxidation of 6-Substituted Benzo(a)Pyrenes by Manganic Acetate. *Abstr. Pap. Am. Chem. Soc.* **1986**, *192*, 11-ORGN.
(10) Goszczynski, S.; Paszczynski, A.; Pastigrigsby, M. B.; Crawford, R. L.; Crawford, D. L. New Pathway for Degradation of Sulfonated Azo Dyes by Microbial Peroxidases of Phanerochaete-Chrysosporium and Streptomyces-Chromofuscus. *J. Bacteriol.* **1994**, *176* (5), 1339–1347.
(11) Lopez, C.; Valade, A. G.; Combourieu, B.; Mielgo, M.; Bouchon, B.; Lema, J. M. Mechanism of enzymatic degradation of the azo dye Orange II determined by ex situ H-1 nuclear magnetic resonance and electrospray ionization-ion trap mass spectrometry. *Anal. Biochem.* **2004**, *335* (1), 135–149.
(12) Spadaro, J. T.; Renganathan, V. Peroxidase-Catalyzed Oxidation of Azo Dyes—Mechanism of Disperse Yellow-3 Degradation. *Arch. Biochem. Biophys.* **1994**, *312* (1), 301–307.
(13) Wariishi, H.; Akileswaran, L.; Gold, M. H. Manganese Peroxidase from the Basidiomycete Phanerochaete-Chrysosporium—Spectral Characterization of the Oxidized States and the Catalytic Cycle. *Biochemistry* **1988**, *27* (14), 5365–5370.
(14) Valli, K.; Gold, M. H. Degradation of 2,4-Dichlorophenol by the Lignin-Degrading Fungus Phanerochaete-Chrysosporium. *J. Bacteriol.* **1991**, *173* (1), 345–352.
(15) Chen, J.-Q.; Wang, D.; Zhu, M.-X.; Gao, C.-J. Study on degradation of methyl orange using pelagite as photocatalyst. *J. Hazard. Mater.* **2006**, *138* (1), 182–186.
(16) Ge, J. T.; Qu, J. H. Degradation of azo dye acid red B on manganese dioxide in the absence and presence of ultrasonic irradiation. *J. Hazard. Mater.* **2003**, *100* (1−3), 197–207.
(17) Liu, R. X.; Tang, H. X. Oxidative decolorization of direct light red F3B dye at natural manganese mineral surface. *Water Res.* **2000**, *34* (16), 4029–4035.
(18) Zhu, M.-X.; Wang, Z.; Zhou, L.-Y. Oxidative decolorization of methylene blue using pelagite. *J. Hazard. Mater.* **2008**, *150* (1), 37–45.
(19) Gutzmer, J.; Beukes, N. J. Mineral paragenesis of the Kalahari manganese field, South Africa. *Ore Geol. Rev.* **1996**, *11* (6), 405–428.
(20) Lu, Y.; Hardin, I. Analysis of sulfonated azo dyes degraded by white rot fungus Pleurotus ostreatus. *AATCC Rev.* **2006**, *6* (1), 31–36.
(21) Tombacz, E.; Csanaky, C.; Illes, E. Polydisperse fractal aggregate formation in clay mineral and iron oxide suspensions, pH and ionic strength dependence. *Colloid Polym. Sci.* **2001**, *279* (5), 484–492.
(22) McKenzie, R. M. The adsorption of lead and other heavy metals on oxides of manganese and iron. *Aust. J. Soil Res.* **1980**, *18*, 61–73.
(23) Pasti-Grigsby, M. B.; Paszczynski, A.; Goszczynski, S.; Crawford, D. L.; Crawford, R. L. Influence of Aromatic-Substitution Patterns on Azo Dye Degradability by Streptomyces Spp and Phanerochaete-Chrysosporium. *Appl. Environ. Microbiol.* **1992**, *58* (11), 3605–3613.
(24) Coen, J. J. F.; Smith, A. T.; Candeias, L. P.; Oakes, J. New insights into mechanisms of dye degradation by one-electron oxidation processes. *J. Chem. Soc., Perkin. Trans. 2* **2001**, *11*, 2125–2129.
(25) Zinder, B.; Furrer, G.; Stumm, W. The coordination chemistry of weathering: II. Dissolution of Fe(III) oxides. *Geochim. Cosmochim. Acta* **1986**, *50*, 1861–1869.
(26) Matocha, C. J.; Sparks, D. L.; Amonette, J. E.; Kukkadapu, R. K. Kinetics and mechanism of birnessite reduction by catechol. *Soil Sci. Soc. Am. J.* **2001**, *65* (1), 58–66.
(27) Laha, S.; Luthy, R. G. Oxidation of Aniline and Other Primary Aromatic-Amines by Manganese-Dioxide. *Environ. Sci. Technol.* **1990**, *24* (3), 363–373.
(28) Ulrich, H. J.; Stone, A. T. Oxidation of Chlorophenols Adsorbed to Manganese Oxide Surfaces. *Environ. Sci. Technol.* **1989**, *23* (4), 421–428.
(29) Zhang, H. C.; Huang, C. H. Oxidative transformation of triclosan and chlorophene by manganese oxides. *Environ. Sci. Technol.* **2003**, *37* (11), 2421–2430.
(30) Bandara, J.; Mielczarski, J. A.; Kiwi, J. 1. Molecular mechanism of surface recognition. Azo dyes degradation on Fe, Ti, and Al oxides through metal sulfonate complexes. *Langmuir* **1999**, *15* (22), 7670–7679.
(31) Zille, A.; Gornacka, B.; Rehorek, A.; Cavaco-Paulo, A. Degradation of Azo Dyes by Trametes villosa Laccase over Long Periods of Oxidative Conditions. *Appl. Environ. Microbiol.* **2005**, *71* (11), 6711–6718.
(32) Huang, P.-K. C.; Kosower, E. M., III. Properties of phenyldiazene. *J. Am. Chem. Soc.* **1968**, *90* (9), 2367–2376.
(33) Kosower, E. M.; Huang, P.-K. C.; Tsuji, T.; Diazenes, V. Aryldiazenes. *J. Am. Chem. Soc.* **1969**, *91* (9), 2325–2329.

ES902305E